ICANS XIV
14th Meeting of the International Collaboration on Advanced Neutron Sources
June 14-19, 1998
Starved Rock Lodge, Utica, IL

Extending the Domain of Time-of-Flight Powder Diffraction Techniques.

Paolo G. Radaelli
ISIS Facility, Rutherford Appleton Laboratory, Chilton Didcot, Oxfordshire, OX11 0QX, UK

ABSTRACT

One of the most significant drawbacks traditionally attributed to the time-of-flight method is its intrinsically limited q-range at low q. For this reason, a significant number of scientific application of neutron powder diffraction have remained almost exclusive domain of constant-wavelength techniques. In this paper, we will discuss a number of possible routes to extend the q-domain of the time-of-flight technique. Some of these methods can be applied to the new instruments which are currently being constructed, with only minor modifications to the detector and software design. We will also discuss an "angular focusing" technique, which would require an altogether different detector concept, but would produce significant advantages both in terms of instrument performances and of q-range.

I. INTRODUCTION

Up to now, the field of neutron powder diffraction has enormously benefited from the complementary nature of time-of-flight (TOF) and constant-wavelength (CW) techniques. Broadly speaking, TOF powder diffraction has concentrated on producing histograms where constant resolution is obtained over relatively narrow d-spacing ranges (Δd = 2-4 Å), possibly extending to very high $q=2\pi/d$ (q is the so-called elastic momentum transfer), whereas CW powder diffraction allows a very large d-spacing range to be accessed on a single histogram (Δd = 20-40 Å), albeit with variable resolution and relatively low q_{Max}. Clearly, there is a significant overlap between the two techniques, but a non-negligible subset of the powder diffraction applications requires either high q_{Max} (e.g., Fourier transform-based methods like pair distribution function analysis, or PDF) or extended d-spacing ranges (e.g., magneto-structural determinations, host/guest problems etc.). However, since in the future the most intense advanced neutron scattering facilities will be pulsed sources, an increasingly large fraction of the available beam time for neutron powder diffraction will be at TOF instrument. If the quality of the demand from the scientific community does not change, this requires the domain of TOF powder diffraction to be progressively extended towards areas which have up to now been regarded as almost exclusive to CW instruments. To this effect, three approaches could be envisaged: 1) Promoting a more effective use of the available solid angle at low 2θ, by making multi-bank indexing and refinements a routine practice for the average user. 2) Extending the q-range of single histograms on individual banks. 3) Combining all the available solid angle in a *single* histogram with *variable* resolution, as it is done on CW diffractometers. The first two approaches can be implemented on thermal-neutron diffractometers using current technology, and are presently guiding the development of new machines like the General Material Diffractometer GEM at ISIS. The feasibility of the third approach, namely for cold-neutron diffractometers, will also be discussed in the present paper.

II. THE MULTI-BANK APPROACH

Most TOF powder diffractometers are equipped with more than one detector bank, and typically have banks at back-scattering, 90 degrees and "low angle" (60-30 degrees), the first two being the most frequently used for high-resolution and special-environment applications, respectively. Although each of these banks is used for particular applications, the *simultaneous* use of all banks is not routine practice. In fact, setting up and successfully completing a multi-histogram Rietveld refinement is a rather complex task, which is undertaken only when the potential benefit of the additional information is clearly perceived. For this reason, simultaneous x-ray and neutron (X&N) refinements are more common than multi-bank refinements, due to the enhanced elemental sensitivity of the X&N technique. Furthermore, the benefit of the additional information at low q is not infrequently offset by the overall increase of χ^2, since the quality of the multi-bank fits is lower than that of single-banks ones. This situation can only be reversed if the bank structure is made *transparent* to the user, in the sense that the TOF-to-d-spacing conversion parameters (e.g., DIFA and DIFC in the GSAS notation[1]) and the instrumental profile parameters are determined once and for all by the instrument scientist and not refined every time. An even more stringent requirement concerns

multi-bank *indexing:* it should be possible to feed the extracted Bragg peak positions to an auto-indexing code and

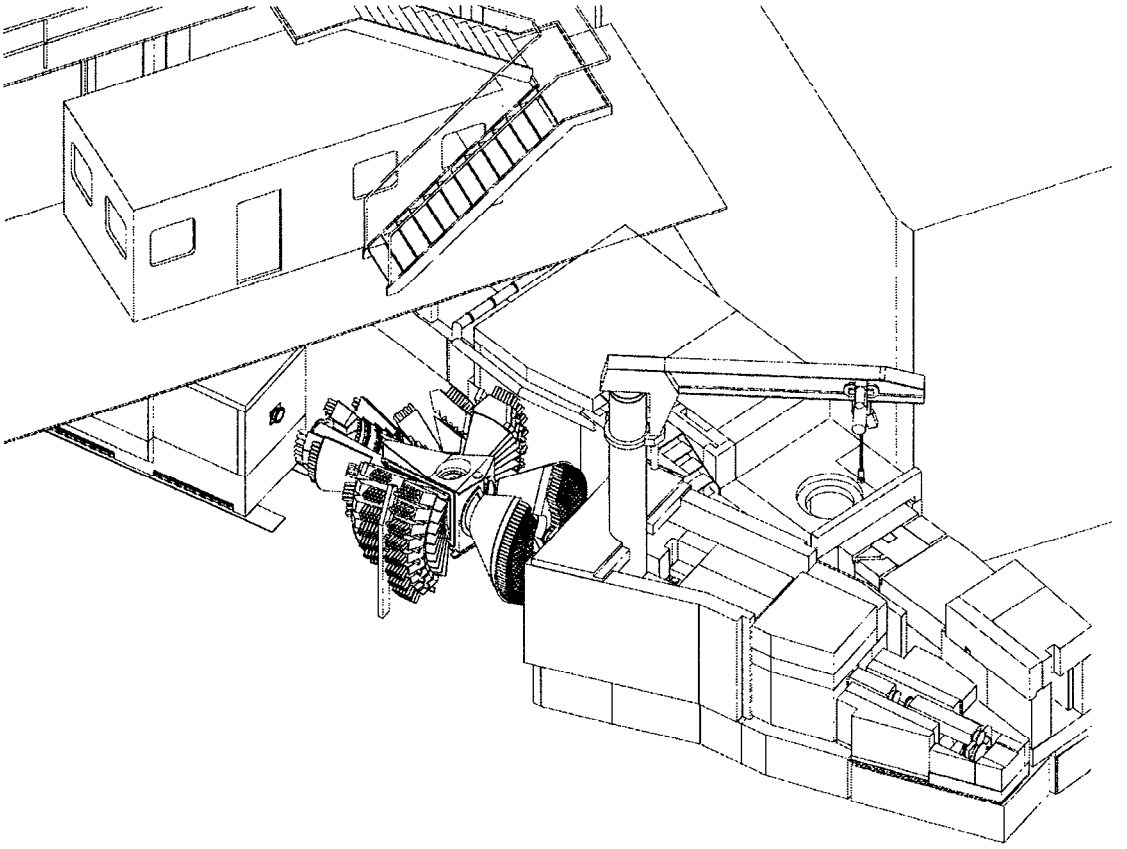

Figure 1: An artist's view of the new high-intensity General Materials Diffractometer GEM, which is presently under construction at ISIS.

obtain good quality factors for the correct solution. Such ambitious goals present major challenges for both the instrument designer and the software developer, and require a different approach to the measurement itself.

Instrument Requirements: Understanding in detail the pulse-shape profile is in itself a major challenge, which is presently best accomplished through analytical expressions like the Ikeda-Carpenter function[2]. However, is unlikely that a profile resulting from the convolution of the Ikeda-Carpenter function with another asymmetric function could be properly modelled. Therefore, all other contribution to the instrumental peak profiles should be well understood, "simple" and symmetric for all banks. The sample size and shape should be accounted for by simple functions. This amounts to constructing instruments with *intrinsic rotational symmetry* around the incident beam. In fact, in addition to the pulse-shape function, the other major source of asymmetry in the peak profiles is the so-called *axial divergence*, which occurs whenever the Debye-Scherrer cones are not geometrically matched with the detector receiving surfaces. The only solution to this problem is to avoid axial asymmetry altogether, by matching the detector elements as close as possible to the Debye-Scherrer rings. This approach has already been implemented in back-scattering (HRPD, POLARIS, OSIRIS), but should become commonplace also for the other detector banks, if a truly user-friendly multi-bank analysis is envisaged. In the development of the new, high-flux General Materials Diffractometer GEM at ISIS, we have been paying close attention to this aspect. The aim of GEM (an artist view of the instrument is shown in Figure 1) is to achieve extremely fast data collection rates with a very wide solid angle coverage at all values of 2θ (see Table I), while still maintaining a sufficiently good resolution in back-scattering (2-3×10^{-3}). Once fully commissioned, GEM will be able to produce data suitable for refinements of complex nuclear and magnetic structures as a function of a rapidly changing variable (temperature, time, etc.). Also, the exceptional stability achieved on the GEM scintillator prototypes (~1×10^{-4}) will allow GEM to excel also in the liquid/amorphous material arena, as well as for measurements of total scattering. Figure 2 shows the calculated peak

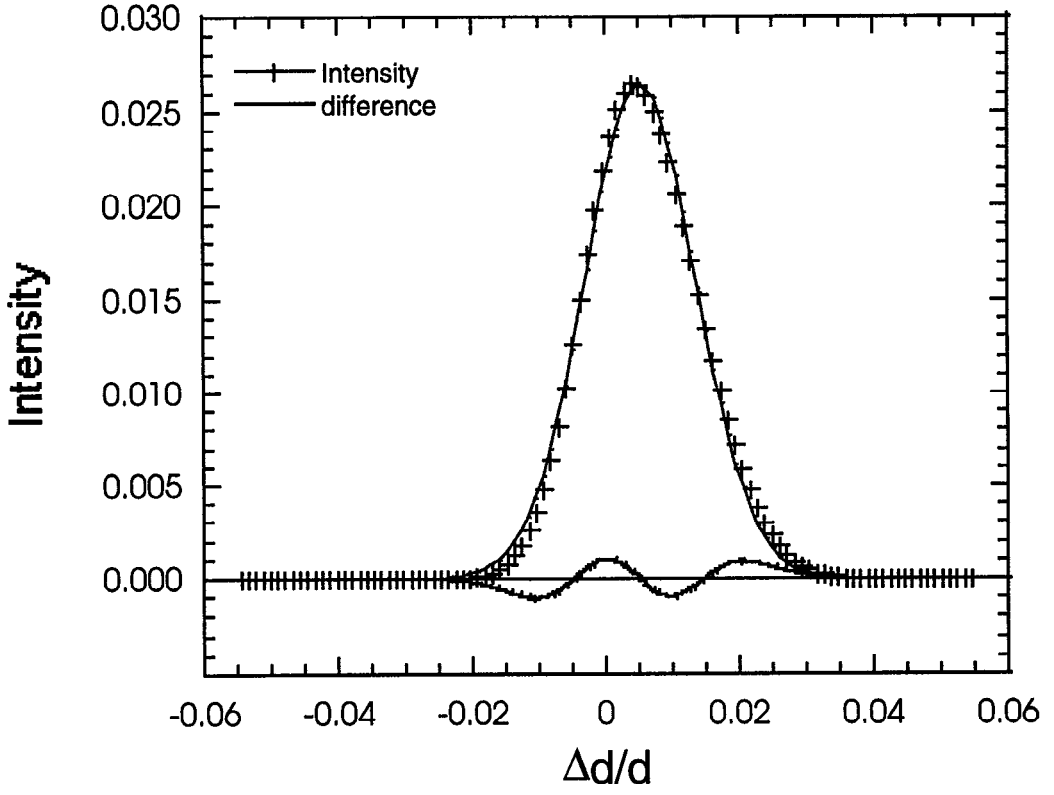

Figure 2: Calculated profile (crosses) and Gaussian fit (continuous line) for a typical setting of GEM-Bank2. Note the asymmetric profile and the shift from the ideal "Bragg" position, due to axial divergence..

profile for the 20-degree bank (GEM-Bank2) assuming that the receiving detector element is a vertical 200mm x 5mm x 5mm parallelepiped. Also shown is the best Gaussian fit to the data. The poor matching between the two curves is clearly evidenced by the difference curve. Note that neither of the two curves peaks at 0 (which is the ideal Bragg value), because the axial divergence not only affects peak *shapes*, but also peak *positions*. The calculation does not include the pulse-shape function, the effect of which is minute at 20 degrees. However, it should be kept in mind that, for higher angle banks, the total profile results from the convolution of these two asymmetric profiles. A quantitative description of the profiles resulting from axial divergence has been developed by Van Laar and Yelon for the case of constant-wavelength diffractometers [3], and has recently been implemented in the Rietveld code GSAS in a slightly modified form [4]. However, a convolution of the Van Laar-Yelon function with the Ikeda-Carpenter function is not currently implemented in any Rietveld code, and would presumably be very difficult to model and calibrated (note that the Van Laar-Yelon profile depends on sample *height*). A simplified description in terms of split functions could be envisaged, but such an approach would prevent absolute cross-bank calibration, because the position of the peak *maximum* (related to the DIFA parameter) depends on the width of the convoluting Gaussian, i.e., on parameters such as sample diameter, strain etc. Figure 3 shows a schematic layout of GEM-Bank2, as it is presently been detailed after performing the aforementioned analysis. The length of the detector elements (80 mm) is such that the width of the Debye-Scherrer rings across the element does not exceed the width of the detector.

Software Requirements.: Making the bank structure transparent to the user requires a change in the traditional layout of the Rietveld input files. The sample contribution to the peak profiles (to be routinely refined) should be kept separate from the instrument contribution. Also, geometric effects such as "effective" sample position (including transparency effects) should be properly taken into account.

Experimental Requirements. Carried to the extreme, the multi-bank approach implies that a *single* scale factor should be refined for all banks. In fact, one may argue that one should refine *no scale factor at all*, since the scale

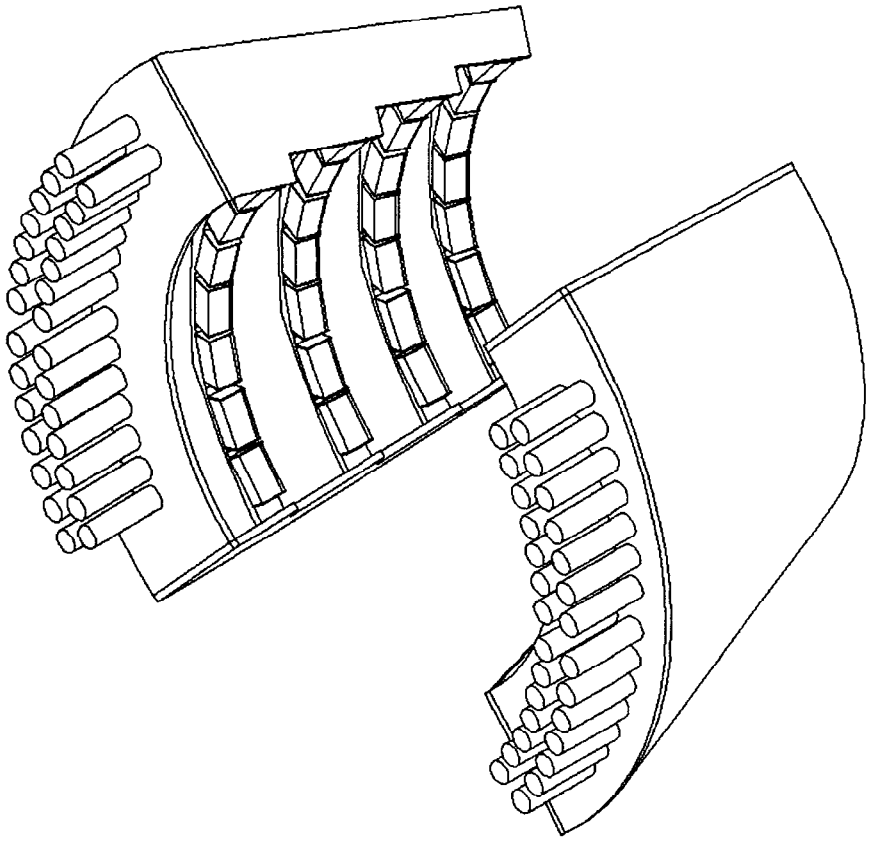

Figure 3: The layout of the 20-degree Bank 2 for GEM. Note the Debye-Scherrer binning over the large elevation angle range.

factor is nothing but a measure of the sample weight, which can obviously be obtained very precisely by other means. Such an approach, if implemented with sufficient accuracy, could have a non-negligible scientific value, especially in problems involving multiple site substitutions. Clearly, this is only possible if absorption, multiple-scattering and vanadium corrections (the latter for efficiency and incident flux) are performed consistently for every measurement. In other words, each measurement should yield *absolute cross sections* (Barns/Sterad/f.u.). This would have the additional benefit of making possible quantitative comparisons between coherent and incoherent scattering. It is noteworthy that absolute cross section measurements are routinely performed on liquid and amorphous materials.

III. THE SINGLE-BANK, NARROW BANDWIDTH APPROACH

Angle-dispersive and wavelength-dispersive techniques significantly differ in the way reciprocal space coverage is achieved. For CW instruments,

$$\Delta q = \frac{4\pi}{\lambda} \cdot \Delta(\sin\theta) \leq \frac{4\pi}{\lambda} = q_{MAX} \quad ; \quad q_{\min} = \frac{4\pi}{\lambda} \cdot \sin\theta_{\min} \tag{1}$$

In other words, for a given wavelength (histogram) there is an intrinsic limit to q_{MAX}, but the value of q_{min} is only dictated by the minimum measured value of the scattering angle. For instance, with a wavelength $\lambda = 2.4$ Å (near-optimum on thermal beams), values of $q_{min} \sim 0.2$ Å^{-1} (d~30 Å) can routinely be achieved Å, while keeping respectably high values of $q_{MAX} \sim 5$ Å^{-1}. The situation is completely different for the TOF technique: for a single bank focused at $2\theta_B$. In fact, for a given time frame,

$$\Delta q = (\hat{q})^2 \cdot \Delta\frac{1}{q} = (\hat{q})^2 \cdot \frac{1}{4\pi \sin\theta_B} \cdot \Delta\lambda \quad = \frac{3957\left[m \cdot \sec^{-1} \cdot \text{Å}\right]}{4\pi \sin\theta_B \cdot L[m]} \times \frac{(\hat{q})^2}{\nu\left[\sec^{-1}\right]} \qquad (2)$$

where $\hat{q} = \sqrt{q_{min} \cdot q_{MAX}}$, L is the flight-path and ν is the repetition rate. In other words, Δq is proportional to the *square* of $\hat{q}$ (logarithmic average of the reciprocal space vector modulus) and *inversely proportional to the repetition rate*, all other parameters being fixed by the instrument geometry. This means, first of all, that it is much easier to cover the reciprocal space efficiently at high q than for CW instruments, which explains the extraordinary success of TOF instruments for applications where a high value of q_{MAX} is required. However, the implication is that low-q coverage is an exercise of diminishing returns, particularly for high-resolution instruments. For instance, for HRPD in back-scattering (L ~100 m; ν 10 Hz; ΔT~100 msec) the typical frame setting (30 msec < T < 130 msec) covers a q-range 2.4 Å^{-1}< q < 10.42 Å^{-1}; Δq = 8.02 Å^{-1}. The next frame setting (130 msec < T < 230 msec) covers 1.36 Å^{-1}< q < 2.40 Å^{-1}, with Δq = 1.04 Å^{-1}.

To a certain extent, these constraints are imposed by the nature of the wavelength-dispersive technique. However, it is possible to obtain extended q-space histograms by carefully choosing the data acquisition strategy. Traditionally, in high-resolution TOF, extended q-data sets are obtained by reducing the repetition rate (see equation (2)). This approach has the disadvantage that the integrated flux, and, as a consequence, the statistical quality of the data, widely vary across the histogram. A better choice is to run the instrument at *high repetition rate* (narrow bandwidth), and accumulate data across the desired q-range by varying $\overline{\lambda}$. This narrow bandwidth (NBW) method is currently employed for cold neutron diffractometers, like OSIRIS, where the typical required d-spacing range (>10 Å) is much bigger than the typical d-spacing window (~2 Å). As an example, Figure 4 shows two low-temperature powder diffraction patterns for the antiferromagnetic compound $La_{0.5}Ca_{0.5}MnO_3$, as obtained on a CW instrument (D2B at the ILL) and on a TOF instrument (OSIRIS at ISIS). For OSIRIS, the complete powder pattern was reconstructed by adding up a series of 8 individual histogram, each with a d-spacing range of 2 Å. In order to estimate the required acquisition times to obtain uniform statistics, we recall that, in the TOF method, the integrated intensity of a Bragg peak is given by the formula:

$$I_{hkl} = N \cdot i(\lambda) \frac{\lambda^4}{32\pi v_0} m_{hkl} \left|F_{hkl}\right|^2 \frac{\Omega}{\sin^3\theta} \qquad (3)$$

where the following symbols are used:

N Number of Unit Cells
$i(\lambda)$ Incident Flux
v_0 Unit Cell Volume
m_{hkl} Reflection Multipliciy
$\left|F_{hkl}\right|^2$ Structure Factor
Ω Detector Solid Angle
θ Bragg angle

Therefore, uniform statistics would be obtained by setting an acquisition time T such that the function $T \cdot i(\lambda) \cdot \lambda^4$ is constant . Note that CW data *do not have uniform statistics*, but are biased at low q due to the Lorentz factor $\frac{1}{\sin 2\theta \cdot \sin\theta}$, which is roughly proportional to $\frac{1}{q^2}$ (the exact q-dependence of the Lorentz factor depends on the wavelength). In order to have the same bias in the TOF method, one would need to operate at constant $T \cdot i(\lambda) \cdot \lambda^2$. Clearly, the details of the scientific case for each experiment may require a different bias, which may

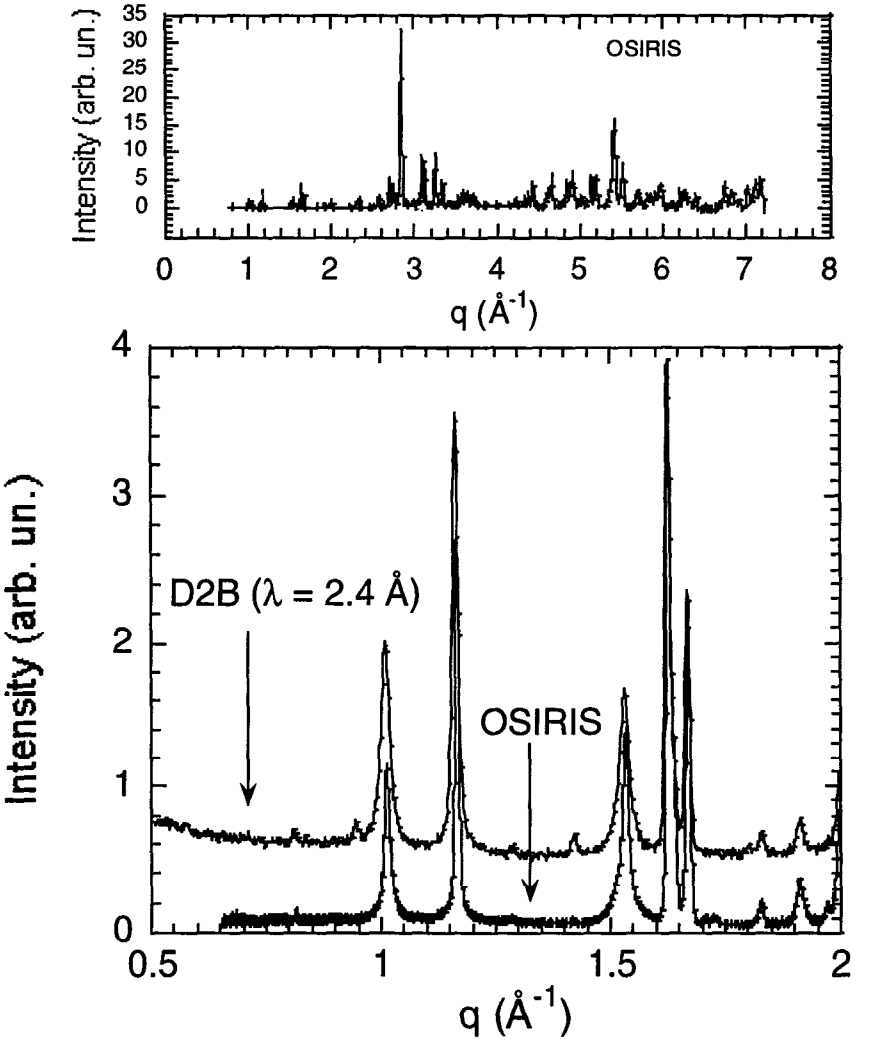

Figure 4: **Top:** Extended q-range histogram for $La_{0.5}Ca_{0.5}MnO_3$ as measured on OSIRIS, by combining data from 8 chopper phase settings. With the λ = 2.4 Å wavelength, D2B has a q-range of ~ 5 Å^{-1}. **Bottom:** Comparison between OSIRIS and D2B (λ = 2.4 Å) in the low-q range for the same compound. Note the better resolution and the absence of contamination in the OSIRIS data.

be achieved with an appropriate acquisition scheme. Figure 5 shows the functions $i(\lambda) \cdot \lambda^4$ and $i(\lambda) \cdot \lambda^2$, for the instrument HRPD at ISIS. It is clear by inspection that, by using a single large bandwidth window, the high-q data are enormously under-sampled, also due to the guide cut-off for epithermal neutrons, and there is potentially a very

significant high-q statistical gain to be obtained by operating the instrument at 50 Hz with variable acquisition times. There is also some under-sampling at long wavelengths for the "CW" bias.

It should be noted that the NBW optimisation is more efficient if a narrow wavelength window is selected. In other words, the NBW method yields the maximum gain in statistics if the instrument is operated at the *source frequency*. However, the efficiency of this mode of operation is reduced by the opening and closing time of the bandwidth-selecting chopper, which normally operates at constant frequency and with a variable aperture. Therefore, the use of the NBW method would be favoured by the development of high-speed choppers.

A distinct *disadvantage* of the NBW method is the fact that not all the final q-range is collected at the same time. Therefore, one would have to wait until the end of the measurement in order to see the low-q data, which significantly hampers the ability of the user to plan ahead in the experiment. A possible solution would be represented by the development of variable-speed choppers, which would "sweep" the required wavelength range many times during the measurements, according to a pre-established distribution. A similar method is employed in the Fourier Diffraction technique (Reference 5). It is noteworthy that the control over the phase of the chopper does not need to be very accurate, since all the data (including the incident spectrum) would be accumulated into an extended time frame, and treated as a single histogram.

IV. ANGLE-DISPERSIVE DATA BY THE TOF TECHNIQUE

The NBW method is a first step to bridge the gap between CW and traditional TOF instruments, since, at least at the low-q end of the spectrum, the bandwidth would only be a fraction of the average wavelength. One may think to go all the way along this line, and investigate the instrument requirements to obtain *angle-dispersive* data with the TOF

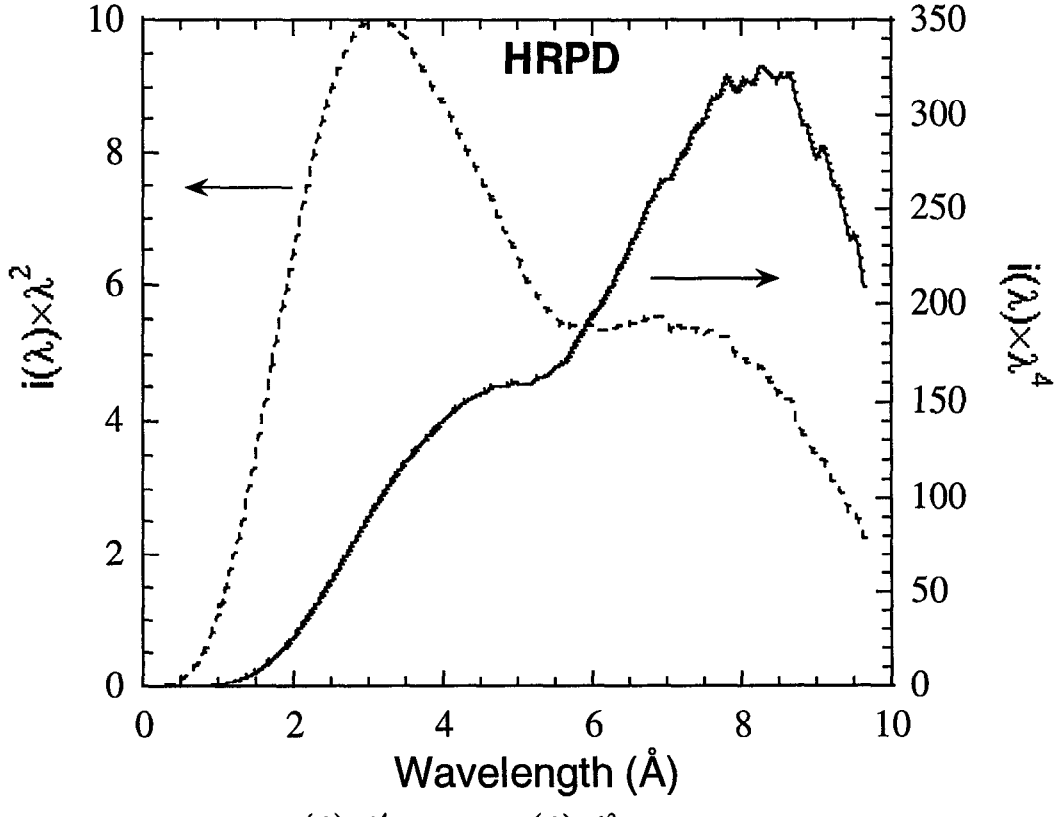

Figure 5: The two functions $i(\lambda)\cdot\lambda^4$ (right) and $i(\lambda)\cdot\lambda^2$ (left) for the instrument HRPD. The reciprocal of these functions is proportional to the data acquisition time for uniform statistics and "CW" statistics, respectively (see text).

method. This is only apparently a contradiction in terms. In fact, as long as the bandwidth is sufficiently small, it is possible to reconstruct a single, angle dispersive data set from TOF data by assigning to each TOF an angular correction (*angular focusing*). Table I shows that angular focusing is the "mirror image" of time focusing with respect to resolution focusing.

Table I: Relationship between different focusing techniques in TOF diffraction.

Technique	Time Focusing (TF)	Resolution Focus. (RF)	Angular Focusing (AF)
Focusing	$\tau \rightarrow \tau \pm \Delta\tau(2\theta)$	$q = q(\tau, 2\theta)$	$2\theta \rightarrow 2\theta \pm \Delta 2\theta(\tau)$
Angular Range	Narrow	Broad (in principle)	Broad
Wavelength Range	Broad	Broad	Narrow
Resolution	Fixed	Fixed	Variable
Histograms Types	Multiple angles	Single/Multiple angles	Multiple Wavelengths

In other words, in the TF technique, the angular range is limited by the need to limit resolution variations across the banks. Likewise, in the AF method, it is the *wavelength* range to be limited by the same requirement. If the "natural" bandwidth of the instrument (given by the source repetition rate through equation (2)) is *broader* than the required bandwidth, multiple wavelength-histograms can be obtained (each with a narrow BW), exactly as for the TF case, where multiple angle-histograms are measured. In principle, the RF focusing method is the best of both worlds, since it could be applied to large detector banks and broad BW. However, in practice, it is impossible to build resolution-focused detectors with very large 2θ ranges, and the RF technique remains confined to individual banks.

In order to assess the viability of the AF method, we need to calculate the fluctuation in resolution across the wavelength band that is focused to a given Bragg angle. To simplify the problem, we use the following expression for the resolution R (Reference 6):

$$R = \left[c^2 + (\delta \cdot \cot\theta)^2\right]^{1/2}, \tag{4}$$

where δ is the angular detector resolution, which includes contributions from the source divergence, sample size and detector element width, and c is the flight-path/pulse width uncertainty, which is, to first approximation, wavelength-independent. In this example, the parameter δ is assumed to be constant, as it would be the case for an instrument with constant secondary flight-path. It is important to stress, however, that this is not a requirement for the applicability of the AF method. The only true requirement is that δ *varies smoothly as a function of* 2θ. In fact, it may be convenient to have a variable secondary flight-path, to approach as much as possible the RF case. This would entail a slowly-varying resolution function, and would allow an even wider band-width to be accepted. In the simple case of δ constant, from equation (4) follows:

$$\frac{\Delta R}{R} = \frac{\delta^2 \cdot \cot\theta \cdot \dfrac{1}{\sin^2\theta}}{c^2 + (\delta \cdot \cot\theta)^2} \cdot \Delta\theta, \tag{5}$$

where $\Delta\theta$ is the angular spread associated to the wavelength band that is re-focused to a single value of θ, and is given by:

$$\Delta\theta = \frac{\Delta\lambda}{\lambda} \cdot \tan\theta \tag{6}$$

By combining equations (5) and (6) we obtain

$$\frac{\Delta R}{R} = \frac{1}{f^2 \cdot \sin^2\theta + \cos^2\theta} \cdot \frac{\Delta\lambda}{\lambda}, \quad \text{where} \quad f^2 = \frac{c^2}{\delta^2} \tag{7}$$

We note that in the special case $c = \delta$ we get $\frac{\Delta R}{R} = \frac{\Delta \lambda}{\lambda}$. Therefore, the resolution fluctuation is comparable to the bandwidth. Clearly, in order to contain the resolution fluctuations, the data may need to be broken up into histograms, each one associated with a narrow BW.

Table II lists the relevant parameters of hypothetical cold-neutron AF instrument with a peak resolution of the order of 0.2%. The geometrical parameters are similar those of OSIRIS at ISIS, but, in our hypothesis, the present back-scattering bank is replaced with a continuous bank (from low- to high-angle) at fixed distance from the sample. The detector elevation angle is assumed to vary from -20° to 20°.

The advantages of this approach are significant: even with a rather conservative elevation angle range, this instrument would have 6.5 times the present OSIRIS solid angle. Also, since OSIRIS currently operates at 25 Hz, the incident flux will be the same, in spite of the narrower bandwidth. In addition, with our resolution fluctuation tolerance, a *single* histogram will be generated for $\lambda \geq 8$ Å. Furthermore, this instrument would have an enormous d-spacing range, whilst still retaining the same *maximum* resolution. The price to pay is that the resolution of this detector will *vary* as a function of 2θ, exactly as for CW instruments. However, this detector can very well coexist with a large-solid angle back-scattering detector, which could be operated either in the usual mode or in the NBW mode, providing constant-resolution data, when needed.

Table II: Geometrical parameters of a hypothetical instrument employing the angular focusing method.

PARAMETER	VALUE
Total Flightpath (m)	40.0
Flightpath/pulse width uncertainty (c)	0.00177
Secondary flightpath (mm)	2000.0
Detector element width (mm)	5.0
Source divergence (rad)	0.00125
Parameter δ	0.00177
Parameter f	1.0
Detector solid angle w. $-20° \leq \phi \leq 20°$ (Sterad)	4.3
"Natural" bandwidth $\Delta\lambda$ @ 50 Hz (Å)	2.0
# of histograms for $\frac{\Delta R}{R} = \pm 10\%$:	
$\lambda = 2$ Å	5
$\lambda = 4$ Å	3
$\lambda = 6$ Å	2
$8 \text{ Å} \leq \lambda \leq 30$ Å	1

V. CONCLUSIONS

As we have shown in this brief discussion, extending the domain of TOF powder diffraction represents a major challenge for future instruments. Some of the possible routes toward the solution of this problem have been outlined. Clearly, with the generation of diffractometers that are presently being built, a major effort should be put into making multi-bank analysis a routine technique. This involves a development both of the instrument design and of the data analysis software. Future instruments may benefit from the narrow-bandwidth and angular-focusing techniques, which will allow them to combine the benefits of the CW and TOF methods. With these instruments, in addition to the normal mode of operation and/or the NBW technique, it should be possible to acquire data with a *single* detector bank, having a very large solid angle and an extended 2θ range One of the major qualities of these instruments is that, similar to the CW instruments, they will produce data across extended q ranges with slowly-varying-resolution. This would make them appealing for a significant segment of the neutron diffraction community, which has so far employed exclusively the CW techniques.

VI. REFERENCES

1 R. B. von Dreele, J. D. Jorgensen, and C. J. Windsor, J.Appl.Cryst. **15**, 581 (1982).

2 S. Ikeda and J. M. Carpenter, Nuc. Instr. and Meth. **A239**, 536 (1985).

3 B. Van Laar and W. B. Yelon, J. Appl. Cryst. **17**, 47 (1984).

4 L. W. Finger, D. E. Cox, and A. P. Jephcoat, J. Appl. Cryst. **27**, 892 (1994).

5 V. L. Aksenov and A. M. Balagurov, Usp. Fizi. Nauk **166**, 955 (1996).

6 J. D. Jorgensen, J. Faber Jr, J. M. Carpenter, *et al.*, J.of Appl. Cryst. **22**, 321 (1989).